2012 18(1) 293-302

DOI: 10.1002/chem.201101413

A Self-Assembled Complex with a Titanium(IV) Catecholate Core as a Potential Bimodal Contrast Agent

Geert Dehaen,[a] Svetlana V. Eliseeva,[a] Kristof Kimpe,[a] Sophie Laurent,[b] Luce Vander Elst,[b] Robert N. Muller,[b, c] Wim Dehaen,[a] Koen Binnemans,[a] and Tatjana N. Parac-Vogt*[a]

Abstract: A ditopic chelating ligand (H_6**4**) that bears catechol and diethylenetriamine-*N*,*N*,*N*′,*N*″,*N*″-pentaacetate (DTPA) has been designed and shown to specifically bind lanthanide(III) ions at the DTPA core ($[Ln(H_2$**4**$)(H_2O)]^-$) and further self-assemble with titanium(IV), thereby giving rise to the formation of a supramolecular metallostar complex with a lanthanide(III)-to-titanium(IV) ratio of 3:1, $[(Ln$**4**$)_3Ti(H_2O)_3]^{5-}$ (Ln = La, Eu, Gd). The efficacy of the metallostar complex as a potential bimodal optical/magnetic resonance imaging (MRI) agent has been evaluated. Nuclear magnetic relaxation dispersion (NMRD) measurements for the $[(Gd$**4**$)_3Ti(H_2O)_3]^{5-}$ complex have demonstrated an enhanced r_1 relaxivity that corresponds to 36.9 $s^{-1}mM^{-1}$ per metallostar molecule at 20 MHz and 310 K, which is a result of a decreased tumbling rate. The ability of the complex to bind to human serum albumin (HSA) was also examined by relaxometric measurements. In addition, upon UV irradiation the $[(Gd$**4**$)_3Ti(H_2O)_3]^{5-}$ complex exhibits broad-band green emission in the range 400–750 nm with a maximum at 490 nm. Taking into account the high relaxivity and luminescence properties, the $[(Gd$**4**$)_3Ti(H_2O)_3]^{5-}$ complex is a good lead compound for the development of efficient bimodal contrast agents.

Keywords: gadolinium · lanthanides · magnetic resonance imaging · self-assembly · titanium

Introduction

Over the last three decades, magnetic resonance imaging (MRI) has gained a great importance and is currently routinely used as a diagnostic tool in various medical procedures. Since its introduction, a continuous interest has grown in the development of more efficient, more tissue-specific, and recently, more responsive contrast agents.[1,2] Complexes of gadolinium(III) ions act as contrast agents for T_1-weighted MR images because they decrease the longitudinal relaxation time T_1 by increasing the relaxation rate of the spins of the surrounding water protons.[3] This enhances the image contrast between normal and diseased tissue or indicates the status of organ function or blood flow.[4] The effectiveness of an MRI contrast agent is expressed in terms of its relaxivity, r_1, which is defined as the longitudinal relaxation rate in s^{-1} measured in a solution of Gd^{III} with a concentration of 1 mM. The currently used contrast agents have relaxivities of about 4 to 5 $mM^{-1}s^{-1}$, but according to the Solomon–Bloembergen theory, relaxivities up to 100 $mM^{-1}s^{-1}$ can be achieved.[5] The water proton relaxivity is mainly characterized by four parameters: the number of water molecules in the first coordination sphere of Gd^{III} (q), the exchange rate for these water molecules (τ_M^{-1}), the relaxation behavior of the electron spin of Gd^{III} (τ_{S1}), and the rotational diffusion of the complex in solution (τ_R).[6] One of the ways to achieve a higher proton relaxivity is to slow down the rotational motion of the contrast agent. This can be achieved by binding the Gd^{III} complex by means of covalent or noncovalent bonds to a large macromolecule such as a polymer or a protein.[7–9] Another approach is achieved by incorporating the Gd^{III} complex into slowly tumbling supramolecular assemblies such as micelles or liposomes.[10–12]

Recently, Livramento et al.[13–15] presented a compound they named metallostar, which is a self-assembled Gd^{III} chelate around a central d-block metal ion. The concept of metallostars as potential MRI contrast agents was initially described by Jacques and Desreux.[16,17] Because of the higher molecular weight of the metallostar compounds, higher proton relaxivities may be obtained after formation of a supramolecular polymetallic complex. Furthermore, these compounds show a lower degree of internal flexibility than Gd^{III} chelates in micelles. The higher rigidity and the multiple Gd^{III} ions within one molecule could also reduce the re-

[a] G. Dehaen, Dr. S. V. Eliseeva, Dr. K. Kimpe, Prof. W. Dehaen, Prof. K. Binnemans, Prof. T. N. Parac-Vogt
Katholieke Universiteit Leuven
Department of Chemistry, Celestijnenlaan 200F
P.O. Box 2404, 3001 Heverlee (Belgium)
E-mail: tatjana.vogt@chem.kuleuven.be

[b] Dr. S. Laurent, Prof. L. Vander Elst, Prof. R. N. Muller
NMR and Molecular Imaging Laboratory
Department of General, Organic and Biomedical Chemistry
University of Mons-Hainaut, 7000 Mons (Belgium)

[c] Prof. R. N. Muller
Center for Microscopy and Molecular Imaging
Rue Adrienne Bolland 8, 6041 Charleroi (Belgium)

Supporting information for this article is available on the WWW under http://dx.doi.org/10.1002/chem.201101413.

quired concentration of the contrast agent. For certain applications of MRI, such as cellular imaging, it is favorable to limit the amount of contrast agents to prevent cell damage.

Catechol is known to act as a bidentate chelating ligand that has a high affinity for metal ions in high oxidation states or with a high charge-to-ionic-radius ratios.[18] As a pioneer of metal–catecholate chemistry, Raymond et al. reported in 1984 that due to its high Lewis acidity, the titanium(IV) ion is able to stabilize the catecholate anion over a broad pH range.[19] At physiological pH, a stable complex ($\log\beta_{130}\approx 60$) is formed by coordination of three catechol entities to a central Ti^{IV} ion.[19,20] Later on, taking advantage of this strong affinity, catechol derivatives have been widely used for synthesis of Ti^{IV} complexes and even as binding agents for TiO_2 nanoparticles.[21–24]

In this paper, we describe the synthesis of a new ligand H_6**4**, which bears a catechol and a diethylenetriaminepentaacetic acid (DTPA) moiety linked together through an amide bond (Scheme 1). The DTPA unit provides a stable chelating environment for Ln^{III} ions ($[Ln(H_2\mathbf{4})(H_2O)]^-$),

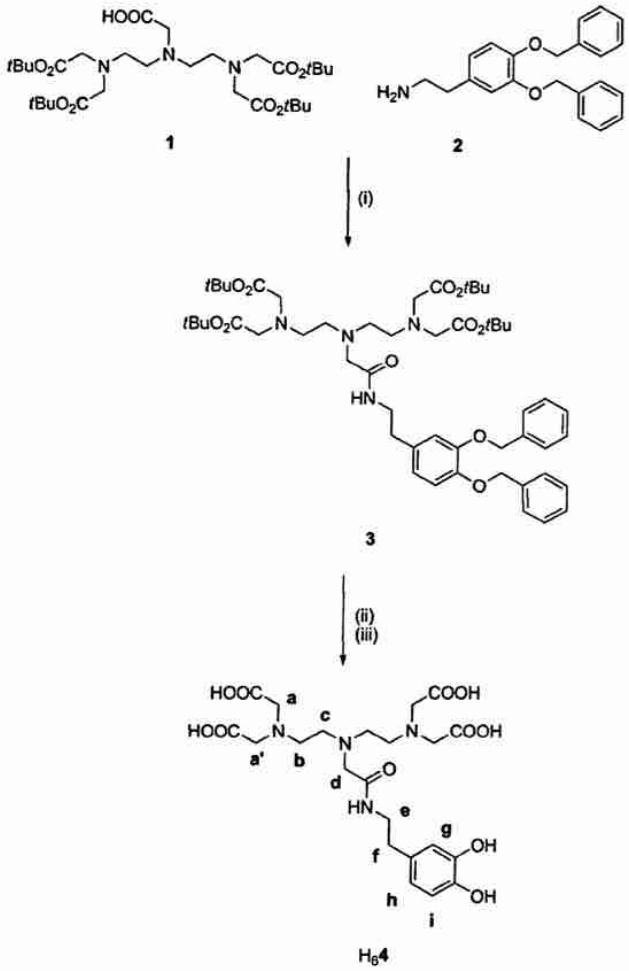

Scheme 1. Synthesis of ligand H_6**4**. Conditions: i) TBTU, dry triethylamine, dry DMF; ii) H_2 gas, Pd/C 5%, methanol; iii) HCl 6N.

whereas catechol is able to self-assemble with a Ti^{IV} ion to form a heteropolymetallic metallostar complex, $[(Ln\mathbf{4})_3Ti(H_2O)_3]^{5-}$ (Ln = La, Eu, Gd). Whereas the $[La(H_2\mathbf{4})(H_2O)]^-$ and $[(La\mathbf{4})_3Ti(H_2O)_3]^{5-}$ complexes allowed ^1H NMR spectroscopic characterization of these metallostars, the Gd^{III} analogues were used for relaxivity studies. In this context, the ability of catechol to bind to human serum albumin (HSA) was examined by relaxometric measurements. To gain more information about the coordination environment and the hydration numbers, the photophysical properties of the corresponding Eu^{III} complexes have also been studied. In addition, to test the feasibility of $[(Gd\mathbf{4})_3Ti(H_2O)_3]^{5-}$ to act as a bimodal contrast agent, its luminescent properties were investigated. Bimodal imaging is presently gaining a great deal of interest since it can take advantage of great spatial, temporal resolution, and unlimited tissue penetration of MRI and high sensitivity of optical imaging.[25–28] Different classes of compounds have been designed as bimodal contrast agents, for example, Gd^{III} chelates derivatized with luminescent dyes or transition-metal complexes,[29–32] as well as functionalized Fe_3O_4,[33] polymer,[34] or silica[35] nanoparticles.

Results and Discussion

The ligand and complexes: The synthesis of the catechol-DTPA-based ligand started from *N,N*-bis(2-{bis[2-(1,1-dimethylethoxy)-2-oxoethyl]amino}ethyl)glycine (**1**),[36] of which only the central carboxylic group remained unprotected. Compound **1** was coupled with 3,4-(dibenzyloxy)phenethylamine (**2**) in the presence of *ortho*-benzotriazol-1-yl-*N,N,N',N'*-tetramethyluronium tetrafluoroborate (TBTU) and dry triethylamine to yield the protected ligand **3**. For the coupling of both entities, an amide bond was chosen because of its high in vivo stability. After deprotection of the phenyl and *tert*-butyl groups, the final ligand H_6**4** was obtained as a white solid (Scheme 1). A proton NMR spectrum of ligand H_6**4** was recorded in D_2O; its peaks corresponded to the labeled molecule (Figure S1 in the Supporting Information). Further, a full assignment was achieved by a two-dimensional COSY experiment (Figure S2 in the Supporting Information).

The electrospray mass spectrum (ESI-MS) in the positive mode showed molecular peaks $[M+H]^+$ and $[M+Na]^+$ at *m/z* 529.6 and 551.9, respectively. Lanthanide(III) complexes were obtained by treating the ligand H_6**4** with a lanthanide(III) chloride (Ln = La, Eu, Gd) under slightly alkaline conditions. All $[Ln(H_2\mathbf{4})(H_2O)]^-$ complexes were purified by Chelex 100 to remove the free lanthanide ions and their purity was checked by a test with an arsenazo indicator solution. Positive-mode ESI-MS of the complexes showed molecular peaks $[M+2Na]^+$ at *m/z* 709.2, 723.0, and 728.0, which correspond to the La^{III}, Eu^{III}, and Gd^{III} complexes, respectively. Complexation of H_6**4** with La^{III} resulted in a significant change in the aliphatic region of the ^1H NMR spectrum. The aliphatic resonances of $[La(H_2\mathbf{4})(H_2O)]^-$ showed a small shift to lower ppm values and a large broadening in

comparison with those of the ligand, while the aromatic resonances remained sharp and unchanged. This indicates the selective coordination of the La^{III} ion to the carboxylic groups of the DTPA moiety. The broadening of the aliphatic resonances is consistent with the occurrence of several interconverting isomers, which is characteristic for lanthanide(III) complexes with DTPA ligands.[37] After heating the solution to 368 K, the aliphatic resonances of $[La(H_24)(H_2O)]^-$ showed severe broadening, whereas the aromatic resonances remained sharp (Figure S3 in the Supporting Information).

To form stable metallostar complexes, Fe^{III}, Ga^{III}, and Ti^{IV} ions were used as central metal ions. However, because mixtures of bis and tris complexes were formed at physiological pH in the presence of Fe^{III} or Ga^{III} ions, these complexes will not be discussed further in this work. In the presence of Ti^{IV}, the color changed from colorless to red, thereby indicating that Ti^{IV} had formed a supramolecular structure with three catechol moieties (Scheme 2).[38] Total-reflection X-ray fluorescence (TXRF) measurements on this complex confirmed a 3:1 ratio of Ln^{III} versus Ti^{IV}. Hence, we can represent the structure of the metallostar compound as $[(Ln4)_3Ti(H_2O)_3]^{5-}$ (Figure 1). In the ^1H NMR spectrum of $[(La4)_3Ti(H_2O)_3]^{5-}$, a shift of the aromatic resonances to-

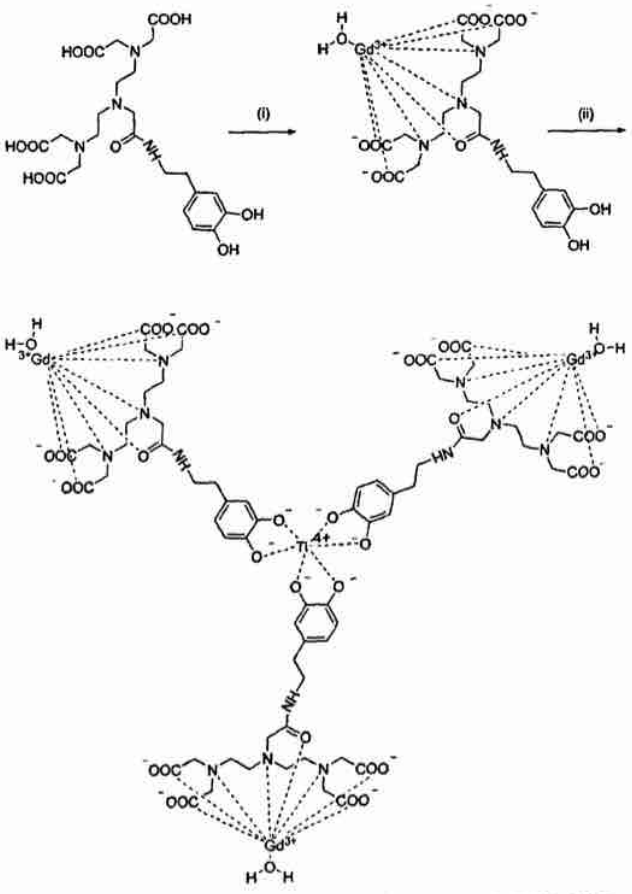

Scheme 2. Formation of the $[(Gd4)_3Ti(H_2O)_3]^{5-}$ complex: i) $GdCl_3{\cdot}6H_2O$, pyridine; ii) $[TiO(acac)_2]$, Na_2CO_3.

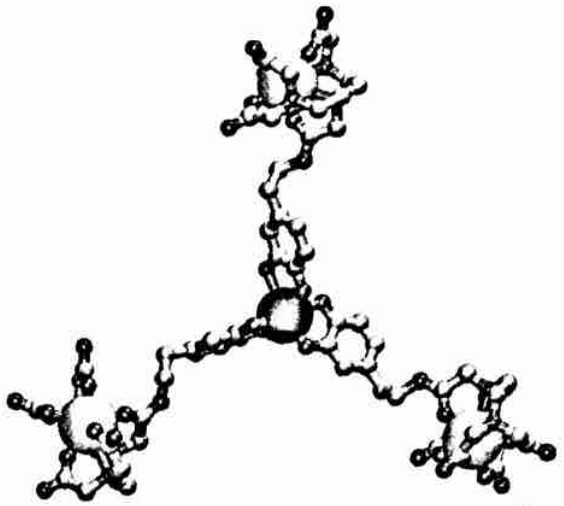

Figure 1. Framework molecular model of the $[(Gd4)_3Ti(H_2O)_3]^{5-}$ complex. Hydrogen atoms have been omitted for clarity.

wards lower ppm values after the complexation of the ligand with Ti^{IV} was observed (Figure S4 in the Supporting Information). The strongest shifts of $\delta = 0.51$ and 0.48 ppm are attributed to protons **g** and **i**, respectively (see Scheme 1 for atom labeling). The aromatic proton **h** underwent a smaller shift of $\delta = 0.23$ ppm. The appearance of only three proton resonances of the aromatic entity of $[(La4)_3Ti(H_2O)_3]^{5-}$ also indicate the formation of only one type of the complex in solution. Although no single crystals suitable for X-ray diffraction analysis could be obtained, the data gained from IR, ESI-MS, NMR, spectroscopic (see below), and TXRF analyses are consistent with the formation of a supramolecular complex with three lanthanide(III) ions and one titanium(IV) ion (Figure 1).

Photophysical properties: The absorption spectrum of ligand H_64 is similar to that of the nonderivatized catechol[39] and displays a band at 281 nm ($\varepsilon = 7185\,M^{-1}cm^{-1}$; Figure 2).

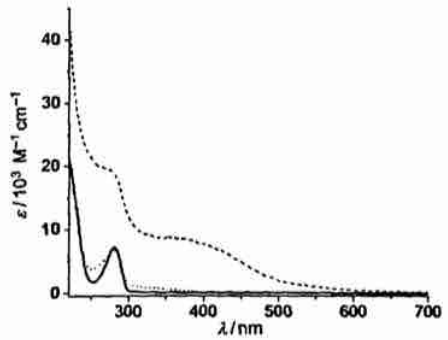

Figure 2. Absorption spectra of ligand H_64 (10^{-4} M, ——), of the complex $[Gd(H_24)(H_2O)]^-$ (10^{-4} M, ••••), and of the metallostar complex $[(Gd4)_3Ti(H_2O)_3]^{5-}$ (3.3×10^{-5} M, -----) in H_2O. The absorption spectra of the Eu^{III} complexes are similar and shown in the Supporting Information (Figure S5).

This band slightly shifts to the blue region and a tail that extends to the red region appears upon complexation with Gd^{III} in $[Gd(H_24)(H_2O)]^-$ ($\varepsilon = 6950\,M^{-1}cm^{-1}$). In the absorption spectrum of $[(Gd4)_3Ti(H_2O)_3]^{5-}$, apart from the ligand-attributed absorption at 277 nm ($\varepsilon = 19375\,M^{-1}cm^{-1}$), the ligand-to-metal charge transfer (LMCT) band appeared at 378 nm ($\varepsilon = 8430\,M^{-1}cm^{-1}$). The position of the LMCT band is typical for Ti^{IV} complexes of catechol.[23,39] Due to the high affinity of Ti^{IV} ions to catechol ligands,[19,21,40] the formation of $[(Gd4)_3Ti(H_2O)_3]^{5-}$ in solution at low concentration remains preserved.

The excitation spectrum of $[Eu(H_24)(H_2O)]^-$ displays a broad band at wavelengths shorter than 350 nm, which is attributed to the electronic transitions of the ligand along with characteristic f–f transitions of the Eu^{III} ion from the $^7F_{0,1}$ levels to $^3P_0$ (307 nm), ^5H_J (313–325 nm), $^5D_4$ (363 nm), ^5G_J, $^5L_7$ (370–390 nm), and $^5L_6$ (396 nm) (Figure 3, top). Upon excitation into the ligand levels at 270–280 nm, $[Eu(H_24)(H_2O)]^-$ exhibits a red luminescence on account of the $^5D_0 \rightarrow {}^7F_J$ ($J = 0$–4) transitions. (Figure 3, bottom). It is well documented that lanthanide luminescence, particularly in the case of Eu^{III}, is very sensitive to the nature of the coordination environment and its symmetry.[41] The integral relative intensities of the transitions are listed in Table S1 in the Supporting Information. The $^5D_0 \rightarrow {}^7F_2$ and $^5D_0 \rightarrow {}^7F_4$ transitions have almost equal integral intensities and represent approximately 40% of the total emission. The highly forbidden $^5D_0 \rightarrow {}^7F_0$ transition has a relatively high integral intensity (13% of $^5D_0 \rightarrow {}^7F_1$ transition), which suggests that the Eu^{III} ion occupies a position with C_n, C_{nv} or C_s symmetry. As expected, the crystal-field splitting patterns of the transitions are similar to the ones observed for other Eu^{III} complexes of DTPA derivatives.[42–44]

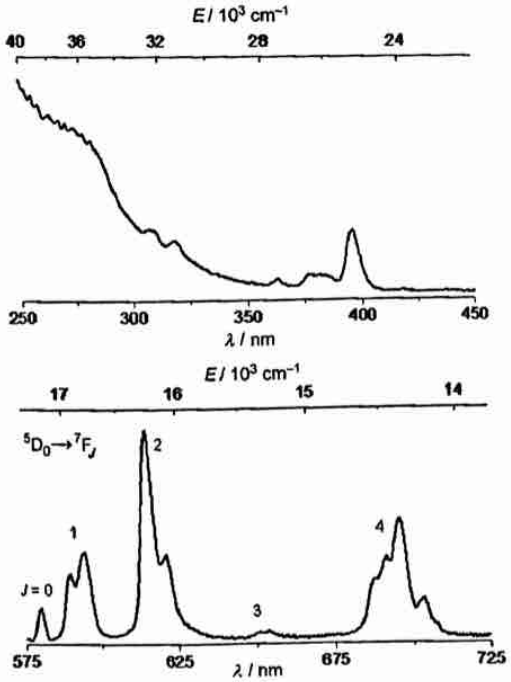

Figure 3. Top: Excitation ($\lambda_{em} = 614$ nm), and (bottom) emission ($\lambda_{ex} = 270$ nm) spectra of the $[Eu(H_24)(H_2O)]^-$ complex in aqueous solution (10^{-4} M).

To determine the number of water molecules coordinated to the Eu^{III} ion, the luminescence lifetimes of the $^5D_0$ level were measured in H_2O ($\tau_{H_2O} = 0.51(1)$ ms) and in D_2O ($\tau_{D_2O} = 1.67(2)$ ms) solutions (Table 1). Calculations were carried out according to the following equation [Eq. (1)]:[45]

Table 1. Photophysical parameters of the $[Eu(H_24)(H_2O)]^-$ complex ($c = 10^{-4}$ M, $\lambda_{ex} = 270$ nm, room temperature).

τ_{obs} [ms]	τ_{rad} [ms][a]	Q^{Eu}_{Eu} [%][a]	Q^{L}_{Eu} [%]	η_{sens} [%][a]
0.51(1)	5.05	10	0.042	0.42(6)

[a] The refractive index was set equal to that of the neat solvents, $n_{H_2O} = 1.34$; $n_{D_2O} = 1.328$. See Equations (2a), (2b), and (3) for definitions.

$$q(Eu) = 1.11 \times (\Delta k - 0.31 - 0.075 \times q^N) \quad (1)$$

in which $q^N = 1$ is the number of coordinated amide groups, thus resulting in $q(Eu) = 1.1$. These results indicate that in $[Eu(H_24)(H_2O)]^-$, the Eu^{III} ions are hydrated by one water molecule and that they are nine-coordinated.

The luminescence quantum yield of $[Eu(H_24)(H_2O)]^-$ under ligand excitation is 0.042%. The intrinsic quantum yield could not be measured because of the low absorption coefficients of the $^5D_0 \leftarrow {}^7F_{0,1}$ transitions, thus it was estimated to be 10% by using the following equations [Eqs. (2a) and (2b)]:

$$Q^{Eu}_{Eu} = \frac{\tau_{obs}}{\tau_{rad}} \quad (2a)$$

$$\frac{1}{\tau_{rad}} = A_{MD,0} \times n^3 \left(\frac{I_{tot}}{I_{MD}}\right) \quad (2b)$$

in which $A_{MD,0}$ is a constant equal to 14.65 s^{-1} and (I_{tot}/I_{MD}) the ratio of the total integrated $^5D_0 \rightarrow {}^7F_J$ emission (here taken as $J = 0$–4) to the integrated intensity of the $^5D_0 \rightarrow {}^7F_1$ magnetic dipole transition. The value of Q^{Eu}_{Eu} is comparable with other hydrated Eu^{III} complexes with 1,4,7,10-tetraazacyclododecane-1,4,7,10-tetraacetic acid (DOTA; 10%)[46] or DTPA (13%)[42] derivatives. However, these complexes display much higher overall quantum yields, 0.4 or 1.9%, respectively, in comparison to a value of 0.042% for $[Eu(H_24)(H_2O)]^-$. This low value is a result of the very inefficient energy transfer from the organic ligand, which could be expected because of the absence of chromophoric groups close to the Eu^{III} ion. Indeed, the sensitization efficiency calculated as the ratio [Eq. (3)]:

$$\eta_{sens} = \frac{Q^{L}_{Eu}}{Q^{Eu}_{Eu}} \quad (3)$$

is equal to only 0.42% for $[Eu(H_24)(H_2O)]^-$. In addition, the formation of a low-lying charge-transfer state in

$[Eu(H_24)(H_2O)]^-$ could be responsible for the luminescence quenching.[47,48]

It is known that the Ti^{IV} ion in an inorganic matrix can exhibit intensive blue, green-blue, or even near-infrared broad-band luminescence (depending on the host matrix), due to $O^{2-}\rightarrow Ti^{IV}$ charge-transfer transitions.[49–53] However, reports that describe the luminescence of Ti^{IV} in complexes with organic ligands are very scarce.[54] On the other hand, whereas Gd–DTPA does not show intraligand (IL) transitions,[55] catechol itself is luminescent and under excitation at 274 nm exhibits broad-band emission centered at 320 nm.[56] To establish the possibility of $[(Gd4)_3Ti(H_2O)_3]^{5-}$ to act as bimodal optical/MRI contrast agent, its luminescence properties were investigated. The excitation spectrum of $[(Gd4)_3Ti(H_2O)_3]^{5-}$ resembles its absorption spectrum, but it is slightly redshifted and it displays two bands at 310 and 400 nm (Figure 4, top). Upon excitation either into the

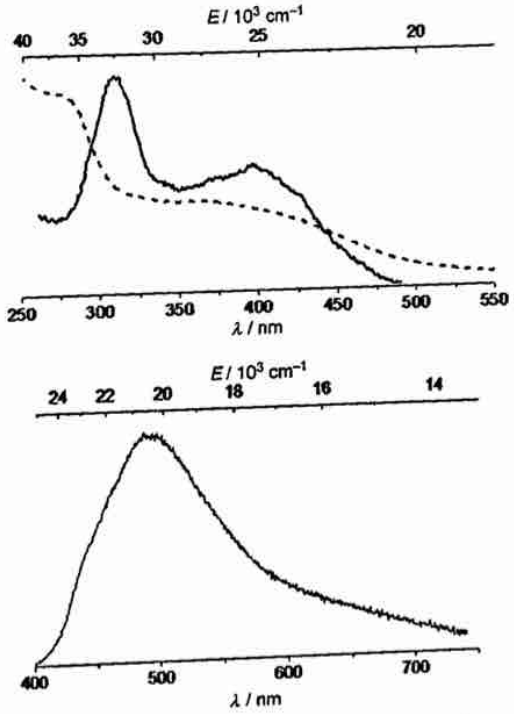

Figure 4. Top: Excitation (solid line, $\lambda_{em}=500$ nm) and superimposed absorption (dashed line) spectra. Bottom: Emission ($\lambda_{ex}=380$ nm) spectrum of $[(Gd4)_3Ti(H_2O)_3]^{5-}$ complex in aqueous solution (3.3×10^{-5} M).

LMCT band at 380 or at 270 nm, $[(Gd4)_3Ti(H_2O)_3]^{5-}$ exhibits a green broad-band emission in the range 400–750 nm with a maximum of 490 nm (Figure 4, bottom), which might be attributed to intraligand and/or ligand-to-Ti^{IV} charge-transfer transitions. However, the absolute quantum yield is relatively low (0.054%).

When it comes to the Eu^{III} derivative, excitation at 380 nm resulted in a similar broad-band emission as in the case of $[(Gd4)_3Ti(H_2O)_3]^{5-}$, however with the characteristic sharp features due to the $^5D_0\rightarrow{}^7F_J$ ($J=0$–4) transitions (Figure S6 in the Supporting Information). Upon excitation at 270 nm, the luminescence spectrum of $[(Eu4)_3Ti(H_2O)_3]^{5-}$ is dominated by the f–f transitions, but the broad emission in the range 400–750 nm still present. The relative integral intensities of $^5D_0\rightarrow{}^7F_2$ and $^5D_0\rightarrow{}^7F_4$ transitions in $[(Eu4)_3Ti(H_2O)_3]^{5-}$ are slightly larger than in $[Eu(H_24)(H_2O)]^-$ (Table S1 in the Supporting Information), whereas the crystal-field splitting of the bands is very similar for the two complexes (Figure S7 in the Supporting Information), thus confirming that the coordination of the catechol moiety to Ti^{IV} does not influence the environment around the Eu^{III} ion. This is further confirmed by measurement of the luminescence lifetimes of the $^5D_0$ level, which remain the same within the limits of the experimental error for $[Eu(H_24)(H_2O)]^-$ and $[(Eu4)_3Ti(H_2O)_3]^{5-}$ in H_2O and D_2O: 0.51(1) versus 0.52(2) ms and 1.67(2) versus 1.65(4) ms, respectively. The Eu^{III} ions are thus monohydrated in $[(Eu4)_3Ti(H_2O)_3]^{5-}$, as evidenced by calculations of $q(Eu)=1.1$ by using Equation (1).

Relaxometric studies: The efficacy of a Gd^{III} complex as an MRI contrast agent is usually assessed through its relaxivity, which is defined as the increase of the proton relaxation rate induced by one mM per liter of complexed Gd^{III}. The relaxivity arises mainly from the contributions of short-distance interactions between the paramagnetic Gd^{III} ion and the coordinated water molecules exchanging with bulk water, the so-called inner-sphere interaction,[57,58] and from the long-distance interactions related to the diffusion of water molecules near the paramagnetic Gd^{III} center, that is, the outer-sphere interaction.[59] The first contribution depends mainly on the number of water molecules coordinated in the first hydration sphere of the complexed ion (q), on the electronic relaxation times of Gd^{III} (τ_{S1} and τ_{S2}), on the residence time of the coordinated water molecules (τ_M), and on the rotational correlation time (τ_R).

The residence time of the coordinated water molecules (τ_M), a key factor of the relaxivity, can be estimated through the analysis of the temperature dependence of the transverse relaxation rate of the ^{17}O NMR spectroscopic resonance of water in the Gd^{III} complex solutions.[60–64] The data obtained for $[(Gd4)_3Ti(H_2O)_3]^{5-}$ are shown in Figure 5.

The theoretical treatment of the experimental data was performed as previously described.[60,61,65] The following parameters were determined: τ_V, the correlation time that modulates the electronic relaxation of Gd^{III}; E_V, the activation energy related to τ_V; B, related to the mean-square of the zero-field splitting energy $\Delta(B=2.4\Delta^2)$; and $\Delta H^{\neq}$ and $\Delta S^{\neq}$, respectively, the enthalpy and entropy of activation of the water-exchange process. The number of coordinated water molecules was set to one in accordance with the data derived from the luminescence lifetime measurements on the Eu^{III} complex, and $A/\hbar$, the hyperfine coupling constant between the ^{17}O nucleus of the bound water molecule and the Gd^{III} ion, was fixed to the typical value of -3.6×10^6 rad s^{-1}. The calculated parameters are shown in Table 2.

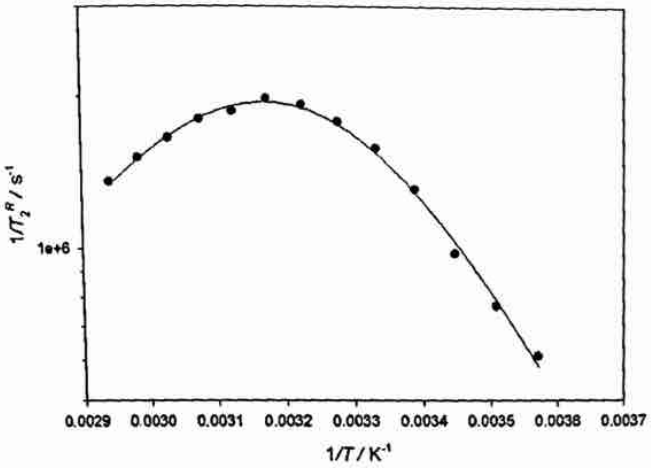

Figure 5. Reduced transverse relaxation rate of ^{17}O ($1/T_2^R = 55.55/(T_2^{para} \times [Gd])$) as a function of the reciprocal of the temperature for $[(Gd4)_3Ti(H_2O)_3]^{5-}$.

Table 2. Parameters obtained by the theoretical adjustment of the ^{17}O transverse relaxation rates versus the reciprocal of the temperature.

	$[(Gd4)_3Ti(H_2O)_3]^{5-}$	Gd–DTPA[a]
τ_M^{310} [ns]	(212 ± 33)	(143 ± 25)
$\Delta H^{\neq}$ [kJ mol^{-1}]	(45.2 ± 0.3)	(51.5 ± 0.3)
$\Delta S^{\neq}$ [J mol^{-1} K^{-1}]	(28.4 ± 0.5)	(52.1 ± 0.6)
$A/\hbar$ [10^6 rad s^{-1}]	−3.6	(−3.4 ± 0.1)
B [10^{20} s^{-2}]	(6.3 ± 0.4)	(2.6 ± 0.1)
τ_V^{298} [ps]	(20 ± 1)	(12.3 ± 0.3)
E_V [kJ mol^{-1}]	(10 ± 4)	(4.5 ± 4.2)

[a] From Ref. [67].

As expected, the calculated value of the water residence time at 310 K is larger than that of the parent compound. Indeed, the replacement of a carboxylic acid function by an amide is known to increase the residence time of the coordinated water molecules. The proton nuclear magnetic relaxation dispersion (NMRD) profiles of the complexes $[Gd(H_24)(H_2O)]^-$ and $[(Gd4)_3Ti(H_2O)_3]^{5-}$ are shown in Figure 6. The NMRD profile of $[Gd(H_24)(H_2O)]^-$ is typical for a low-molecular-weight complex, whereas the profile of $[(Gd4)_3Ti(H_2O)_3]^{5-}$ has a hump around 20 MHz, which is typical of a higher-molecular-weight complex.

The theoretical adjustment of the NMRD profiles takes into account the inner-sphere[57,58] and the outer-sphere[59] contributions to the paramagnetic relaxation rate. Some parameters were fixed during the fitting procedure: q, the number of coordinated water molecules ($q=1$); d, the distance of closest approach ($d=0.36$ nm); D, the relative diffusion constant ($D=3.3\times10^{-9}$ m^2 s^{-1} for $[Gd(H_24)(H_2O)]^-$ and 3.0×10^{-9} m^{2}s^{-1} for $[(Gd4)_3Ti(H_2O)_3]^{5-}$);[66] τ_M^{310}, the water residence time was set to the value determined by ^{17}O NMR spectroscopy; and r, the distance between the Gd^{III} ion and the proton nuclei of water ($r=0.31$ nm). The results of these fittings are shown in Table 3 and Figure 6.

The τ_{SO} values at 310 K are close to that of the Gd–DTPA complex, and as expected, the τ_R value of $[Gd(H_24)(H_2O)]^-$ is larger than the value for the Gd–DTPA complex. The τ_R value of $[(Gd4)_3Ti(H_2O)_3]^{5-}$ agrees with the size of the complex and is responsible of the enhanced relaxivity. It should be emphasized that the relaxivity expressed in mM per liter of the $[(Gd4)_3Ti(H_2O)_3]^{5-}$ complex is 36.9 s^{-1} mM^{-1} at 20 MHz and 37.7 s^{-1} mM^{-1} at 60 MHz and 310 K.

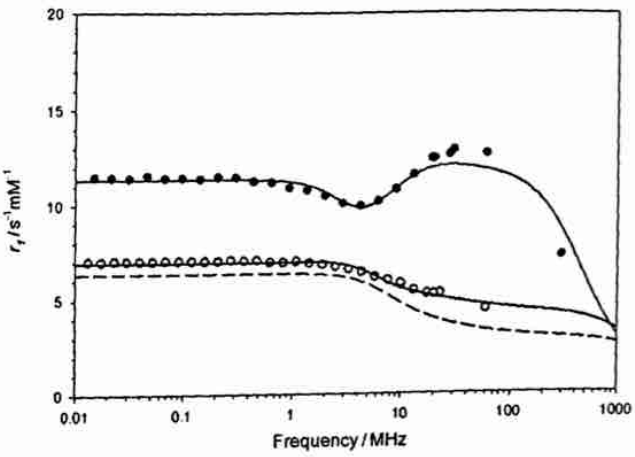

Figure 6. ^1H NMRD relaxivity profiles of $[Gd(H_24)(H_2O)]^-$ (○) and $[(Gd4)_3Ti(H_2O)_3]^{5-}$ (●) in water at 310 K. The relaxivity is expressed by mM per liter of Gd^{III}. The solid lines correspond to the theoretical fittings of the data points. The dashed line corresponds to the fitting of Gd–DTPA data.

Table 3. Parameters obtained by the theoretical adjustment of the proton NMRD data in water at 310 K.

	Gd–DTPA[a]	$[Gd(H_24)(H_2O)]^-$	$[(Gd4)_3Ti(H_2O)_3]^{5-}$
τ_M^{310} [ns][b]	143	212[c]	212
τ_R^{310} [ps]	(54 ± 14)	(104 ± 24)	(371 ± 6)
τ_{SO}^{310} [ps]	(87 ± 3)	(69 ± 1)	(108 ± 1)
τ_V^{310} [ps]	(25 ± 3)	(29 ± 2)	(46 ± 2)
r_1 [s^{-1} mM^{-1}] at 20 MHz	(3.8 ± 0.2)	(5.2 ± 0.3)	(12.3 ± 0.6)

[a] From Ref. [67]. [b] τ_M^{310} was fixed to the value obtained by ^{17}O relaxometry. [c] Fixed to the value obtained for $[(Gd4)_3Ti(H_2O)_3]^{5-}$.

The interaction of a small Gd^{III} complex with human serum albumin (HSA) results in an increase of the paramagnetic relaxation rate as a result of the increase of its rotational correlation time. The change of the observed relaxation rate depends on the intensity of the magnetic field and on the proportion of bound contrast agents, and therefore, on the strength of the interaction. The proton NMRD profiles of the paramagnetic relaxation rate of solutions that contain 1 mM per liter of complexed Gd^{III} and 4% of HSA are shown in Figure 7.

The slight increase of paramagnetic relaxation rate in the presence of HSA is partly explained by the viscosity increase induced by HSA (0.87 MPa s^{-1} with HSA relative to 0.69 MPa s^{-1} without HSA at 310 K). This change of viscosity results in an increased value of τ_R and a decreased value of the relative diffusion constant D. Theoretical fittings performed with the parameters of the free Gd^{III} complexes, but which take into account these viscosity effects on τ_R and D,

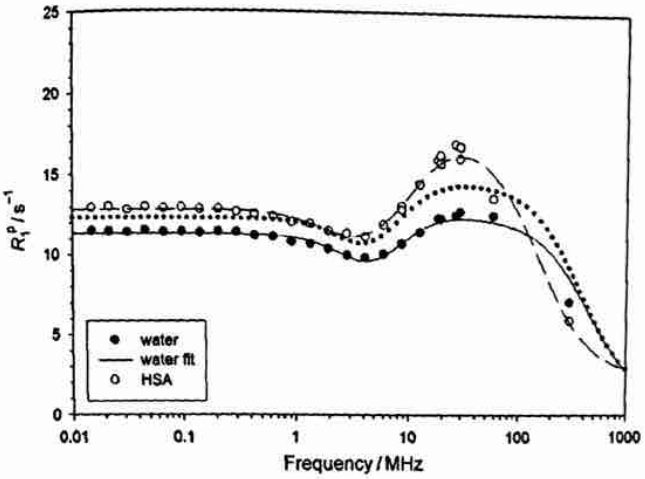

Figure 7. Proton paramagnetic relaxation rate of solutions of $[(Gd4)_3Ti(H_2O)_3]^{5-}$ (1 mM) in water and in aqueous solution of HSA (4%, ○=HSA, ●=water, ——=water fit). The dashed line through the data obtained in HSA is drawn to guide the readers' eyes. The dotted line represents the data calculated, when the viscosity increase is taken into account.

are shown in Figure 7. The data indicate that the presence of HSA does not induce significant modifications. This result was confirmed by the analysis of the paramagnetic proton relaxation rate of solutions that contain 4% of HSA and increasing amounts of $[(Gd4)_3Ti(H_2O)_3]^{5-}$ (Figure 8). The slight increase in paramagnetic relaxation over the concentration range investigated does not indicate the presence of a significant interaction between $[(Gd4)_3Ti(H_2O)_3]^{5-}$ and HSA.

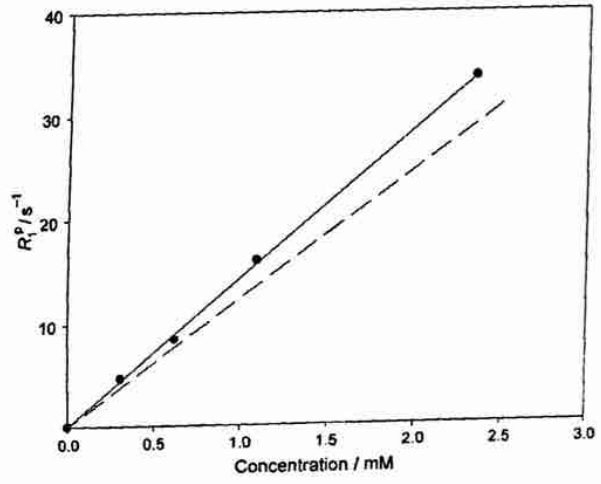

Figure 8. Proton paramagnetic relaxation rate of solutions of $[(Gd4)_3Ti(H_2O)_3]^{5-}$ in an aqueous solution of HSA (4%, ●) at 20 MHz and 310 K. The dashed line represents the data obtained in water (---).

Conclusion

We have demonstrated that a new ditopic DTPA–catechol ligand is able to bind lanthanide(III) ions, $[Ln(H_24)(H_2O)]^-$, and further self-assemble with Ti^{IV}, thereby giving rise to stable metallostar molecules, $[(Ln4)_3Ti(H_2O)_3]^{5-}$. The formation of such a supramolecular complex in case of the Gd^{III} analogue induces a decrease of the tumbling rate by a factor of 4 to 7.4 relative to the monomer and currently used commercial MRI contrast agent Gd–DTPA (Magnevist), respectively. This, in turn, leads to an enhanced r_1 relaxivity up to 12.3 s^{-1} mM^{-1} per Gd^{III} ion at 20 MHz and 310 K that corresponds to 36.9 s^{-1} mM^{-1} per metallostar molecule. In addition to these high relaxivities, the $[(Gd4)_3Ti(H_2O)_3]^{5-}$ complex shows interesting photophysical properties. Under UV excitation, the Gd^{III}–Ti^{IV} metallostar exhibits broad-band green emission with a quantum yield of 0.054%. Although the latter value is rather low, the ligand was not specifically optimized to give highly luminescent complexes. However, appropriate functionalization should make such ditopic ligands promising candidates for the successful design of bimodal optical/MRI contrast agents.

Experimental Section

Materials: Reagents were obtained from Aldrich Chemical (Bornem, Belgium) and Acros Organics (Geel, Belgium) and were used without further purification. Gadolinium(III) chloride hexahydrate was obtained from GFS Chemicals (Powell, Ohio, USA).

Synthesis of *N,N*-bis[(*tert*-butoxycarbonyl)methyl]-2-bromoethylamine:[68] Powdered $KHCO_3$ (19.2 g, 192 mmol, 2.6 equiv) was added to *tert*-butyl bromoacetate (33 g, 173 mmol, 2.3 equiv) dissolved in DMF (150 mL). The suspension was cooled to 0°C and ethanolamine (4.6 mL, 75 mmol, 1 equiv) was added dropwise over a period of five minutes. The reaction mixture was stirred at 0°C for 30 min and then for 24 h at room temperature. The semisolid residue obtained after removal of the solvent was dissolved in a sodium hydrogen carbonate solution and extracted three times with diethyl ether. The combined ether layers were then washed with brine, dried over $MgSO_4$, and evaporated to give crude *N,N*-bis-[(*tert*-butoxycarbonyl)methyl]-2-ethanolamine as an oil (≈18.6 g, 86%). This crude dialkylated product was dissolved in dichloromethane (200 mL), and triphenylphosphine (23.5 g, 89.6 mmol, 1.4 equiv) was added. The solution was cooled to 0°C and solid *N*-bromosuccinimide (NBS; 15.95 g, 89.6 mmol, 1.4 equiv) was slowly added. The reaction was continued for 2 h. The solvent was evaporated to yield a semisolid residue, which was triturated three times with ether, and the remaining solid was separated. The combined ether layers were concentrated and passed through a column of silica using hexane/ether (5:1) as eluent, which resulted in a yellow oil (18.5 g, 82%). R_f=0.36 (5:1 hexane/ether); ^{1}H NMR (300 MHz, $CDCl_3$): δ=1.45 (s, 18H; *tert*-butyl CH_3), 3.1 (t, 2H; $BrCH_2CH_2N$), 3.4 (t, 2H; $BrCH_2CH_2N$), 3.5 ppm (s, 4H; (*tert*-butoxycarbonyl-CH_2)$_2$N); ESI-MS: *m/z* calcd for $C_{14}H_{28}BrNO_4$ [*M*]: 375.3 $[M+Na]^+$; found: 375.6.

Synthesis of 1:[69] Benzyl glycinate *p*-toluenesulfonate (2 g, 6 mmol, 1 equiv) was dissolved in diethyl ether (40 mL), and an Na_2CO_3 solution (1.89 g, 18 mmol, 3 equiv) in water (40 mL) was added. The ether layer was separated from the water layer, dried, and evaporated to yield glycine benzyl ester (0.5 g). This product is very unstable, and was therefore immediately used in the next synthesis step. A phosphate buffer (10 mL, 2M, pH 8) was added to a solution of glycine benzyl ester (0.430 g, 2.6 mmol, 1 equiv) and *N,N*-bis[(*tert*-butoxycarbonyl)methyl]-2-bromoethylamine (2 g, 5.7 mmol, 2.2 equiv) in CH_3CN (20 mL), and the mixture was stirred for 24 h. The suspension was filtered and the organic layer was separated from the water layer, dried, and evaporated. To remove the remaining inorganic salts, the crude product was redissolved in chloroform, filtered, and evaporated again. The yellow oil was passed through a column of silica using a mixture of $CHCl_3$/MeOH/NH_3 150:3:1

as eluent to afford 1.2 g of benzyl-protected product. R_f=0.2 (50:1 chloroform/methanol).

The product was dissolved in methanol (10 mL), then Pd/C 5% (0.14 g) was added, and the suspension was stirred at room temperature under a hydrogen atmosphere for 24 h. The mixture was filtered over Millipore FH 0.45 μm. The solvent was evaporated to yield a highly viscid yellow oil (0.98 g, 61%). ^{1}H NMR (300 MHz, $CDCl_3$): δ=1.45 (s, 36H; *tert*-butyl CH_3), 3.19 (t, 4H; C(O)OHCH$_2$NCH_2CH$_2$N), 3.48 (s, 8H; NCH_2C(O)O*t*Bu), 3.54 (t, 4H; C(O)OHCH$_2$NCH$_2$CH_2N), 4.34 ppm (s, 2H; NCH_2C(O)OH); ESI-MS: *m/z* calcd for $C_{30}H_{55}N_3O_{10}$ [*M*]: 640.8 [*M*+Na]$^+$; found: 641.0.

Synthesis of benzyl- and *tert*-butyl-protected catechol derivative 3: Compound **1** (618 mg, 1 mmol) was dissolved in dry DMF (20 mL). Dry triethylamine (0.5 mL, 0.36 g, 3.6 mmol) and *o*-benzotriazol-1-yl-*N*,*N*,*N*',*N*'-tetramethyluronium tetrafluoroborate (481.5 mg, 1.5 mmol) were added, and the mixture was stirred for 10 min at room temperature. Compound **2** (370 mg, 1 mmol) was then added to the solution. The reaction mixture was stirred at room temperature and followed by TLC through observation of the depletion of free 3,4-(dibenzyloxy)phenethylamine (R_f=0.4) with the eluent CH_2Cl_2/CH_3OH/NH_4OH (9:1:0.1). DMF was then removed by vacuum evaporation. The crude product was washed and phase separated in ethyl acetate (40 mL) with a sodium hydrogen carbonate and saturated sodium chloride solution. The crude yellow oil was passed through a column of silica using CH_2Cl_2→CH_2Cl_2/MeOH 50:1 as eluent. Evaporation of the solvent gave **3** as a yellow oil (0.697 g, 75%). ^{1}H NMR (300 MHz, $CDCl_3$): δ=1.40 (s, 36H; *tert*-butyl), 2.6–2.8 (m, 4H; NCH_2), 3.0 (s, 2H; NCH_2CO), 3.0–3.1 (m, 4H; NCH_2), 3.43 (s, 8H; NCH_2COO*t*Bu), 3.99 (m, 4H; PhCH_2CH_2NH), 5.12 (s, 4H; PhCH_2OPh), 6.7–7.0 (m, 3H; Ph), 7.3–7.5 ppm (m, 10H; Ph); ^{13}C NMR (75 MHz, $CDCl_3$): δ=28.1 (CH_3), 39.4 (CH_2), 40.9 (CH_2), 52.2 (CH_2), 53.8 (CH_2), 55.4 (CH_2), 55.8 (CH_2), 71.3 (CH_2), 71.5 (CH_2), 81.0 (C), 115.4 (CH), 115.8 (CH), 121.7 (CH), 127.4 (CH), 127.7 (CH), 128.4 (CH), 133.2 (CH), 137.5 (CH), 147.4 (C), 149.0 (C), 170.56 (CO), 170.47 ppm (CO); ESI-MS: *m/z* calcd for $C_{52}H_{76}N_4O_{11}$ [*M*]: 934.2 [*M*+H]$^+$, 956.2 [*M*+Na]$^+$; found: 934.0 [*M*+H]$^+$, 956.4 [*M*+Na]$^+$.

Synthesis of *tert*-butyl-protected catechol derivative: Product **3** was dissolved in MeOH (20 mL), and Pd/C 5% (0.5 g) was added. The suspension was stirred over 5 h under a hydrogen atmosphere at room temperature. The mixture was filtered over celite and evaporated to yield a yellow oil (0.338 g, 60%). ^{1}H NMR (300 MHz, $CDCl_3$): δ=1.44 (s, 36H; *tert*-butyl), 2.6–2.8 (m, 4H; NCH_2), 3.0–3.1 (m, 4H; NCH_2), 3.34 (s, 8H; NCH_2COO*t*Bu), 3.48 (s, 2H; NCH_2CO), 3.98 (m, 4H; PhCH_2CH_2NH), 6.5–6.9 ppm (m, 3H; Ph); ^{13}C NMR (75 MHz, $CDCl_3$): δ=28.1 (CH_3), 38.6 (CH_2), 40.9 (CH_2), 47.9 (CH_2) . 53.8 (CH_2), 55.4 (CH_2), 55.9 (CH_2), 80.8 (C), 115.4 (CH), 116.5 (CH), 120.5 (CH), 131.1 (CH), 143.2 (CH), 143.9 (CH), 170.7 (CO), 170.8 ppm (CO); ESI-MS: *m/z* calcd for $C_{38}H_{64}N_4O_{11}$ [*M*]: 753.0 [*M*+H]$^+$, 776.0 [*M*+Na]$^+$; found: 753.0 [*M*+H]$^+$, 776 [*M*+Na]$^+$.

Synthesis of catechol derivative $H_6$4: The *tert*-butyl-protected catechol derivative was dissolved in 6N HCl (10 mL). The mixture was stirred at room temperature for 1 h and then washed with CH_2Cl_2 (2×10 mL). The aqueous solution was concentrated in vacuo and the final compound was obtained as a white solid (223 mg, 91%). ^{1}H NMR (300 MHz, D_2O): δ= 2.63 (t, 2H; PhCH_2CH$_2$CONH), 2.96 (t, 4H; NCH_2), 3.26 (t, 2H; CONHCH_2CH$_2$Ph), 3.39 (t, 4H; NCH_2), 3.46 (s, 2H; NCH_2CO), 3.81 (s, 8H; NCH_2COOH), 6.63 (d, 1H; Ph), 6.76 (s, 1H; Ph), 6.81 ppm (d, 1H; Ph); ^{13}C NMR (100 MHz, D_2O): δ=33.69, 40.36, 50.26, 52.08, 55.47, 55.64, 116.28, 116.80, 121.30, 132.03, 142.37, 143.85, 169.66, 170.31 ppm; IR: $\tilde{\nu}$=1733 (CO free acid), 1670 (CO amide), 1194 cm^{-1} (Ar–CO stretch); elemental analysis calcd (%) for $C_{22}H_{28}O_{11}N_4Na_4(H_2O)_4$: C 38.38, H 5.27, N 8.14; found: C 38.66, H 5.56, N 8.36; ESI-MS: *m/z* calcd for $C_{22}H_{32}N_4O_{11}$ [*M*]: 528.5 [*M*+H]$^+$; found: 529.1.

Synthesis of lanthanide(III) complexes: The lanthanide(III) complexes of ligand $H_6$4 were synthesized according to a general procedure. A solution of hydrated $LnCl_3$ salt (1.05 equiv) in H_2O was added to ligand $H_6$4 (1 equiv) dissolved in pyridine, and the mixture was heated at 70°C for 3 h. The solvents were evaporated under reduced pressure and the crude product was then heated to reflux in ethanol for 1 h. After cooling to room temperature, the complex was filtered off and dried in a vacuum. The absence of free lanthanide ions was checked by using an arsenazo indicator.

Lanthanum(III) complex [La($H_2$4)(H_2O)]$^-$: Yield: 78%; IR: $\tilde{\nu}$=1616 (amide I), 1583 (COO^- asym. stretch), 1405 cm^{-1} (COO^- sym. stretch); ESI-MS: *m/z* calcd for $C_{22}H_{28}LaN_4O_{11}$ [*M*]: 709.4 [*M*+2Na]$^+$; found: 709.2.

Europium(III) complex [Eu($H_2$4)(H_2O)]$^-$: Yield: 84%; IR: $\tilde{\nu}$=1607 (amide I), 1582 (COO^- asym. stretch), 1409 cm^{-1} (COO^- sym. stretch); ESI-MS: *m/z* calcd for $C_{22}H_{28}EuN_4O_{11}$ [*M*]: 722.4 [*M*+2Na]$^+$, found 723.0.

Gadolinium(III) complex [Gd($H_2$4)(H_2O)]$^-$: Yield: 55%; IR: $\tilde{\nu}$=1617 (amide I), 1586 (COO^- asym. stretch), 1409 cm^{-1} (COO^- sym. stretch); ESI-MS: *m/z* calcd for $C_{22}H_{28}GdN_4O_{11}$ [*M*]: 727.7 [*M*+2Na]$^+$; found: 728.0.

Synthesis of titanium(IV)–lanthanide(III) complexes:[38] [TiO(acac)$_2$] (1 equiv; acac=acetylacetonate) and Na_2CO_3 (6 equiv) were added to a solution of [Ln($H_2$4)(H_2O)]$^-$ (3 equiv) in H_2O, and the mixture was stirred at room temperature for 24 h. The color of the mixture immediately changed to red, thereby indicating complexation of catechol to the Ti^{IV} ion. The solution was concentrated, redissolved in a small amount of methanol, and precipitated with acetone. Finally, the complex was filtered off and dried in vacuum.

Titanium(IV)–lanthanum(III) complex [(La4)$_3$Ti(H_2O)$_3$]$^{5-}$: Yield: 68%. IR: $\tilde{\nu}$=1617 (amide I), 1577 (COO^- asym. stretch), 1397 cm^{-1} (COO^- sym. stretch); ESI-MS: *m/z* calcd for $C_{66}H_{78}La_3N_{12}O_{33}Ti$ [*M*]: 709.3 [*M*+4Na+4H]$^+$; found: 709.3; TXRF ratio (La/Ti): 2.92.

Titanium(IV)–europium(III) complex [(Eu4)$_3$Ti(H_2O)$_3$]$^{5-}$: Yield: 71%; IR: $\tilde{\nu}$=1617 (amide I), 1578 (COO^- asym. stretch), 1398 cm^{-1} (COO^- sym. stretch); ESI-MS: *m/z* calcd for $C_{66}H_{78}Eu_3N_{12}O_{33}Ti$ [*M*]: 297.6 [*M*+126H]$^{7+}$; found: 297.7; TXRF ratio (Eu/Ti): 2.92.

Titanium(IV)–gadolinium(III) complex [(Gd4)$_3$Ti(H_2O)$_3$]$^{5-}$: Yield: 66%; IR: $\tilde{\nu}$=1615 (amide I), 1577 (COO^- asym. stretch), 1396 cm^{-1} (COO^- sym. stretch); ESI-MS: *m/z* calcd for $C_{66}H_{78}Gd_3N_{12}O_{33}Ti$ [*M*]: 1098.0 [*M*+3Na+4H+2H_2O]$^{2+}$, 1129.0 [*M*+5Na+2H+3H_2O]$^{2+}$; found: 1098.0 [M+3Na+4H+2H_2O]$^{2+}$, 1129.6 [*M*+5Na+2H+3H_2O]$^{2+}$; TXRF ratio (Gd/Ti): 2.78.

Instruments: Elemental analysis was performed by using a CE Instruments EA-1110 elemental analyzer. ^{1}H and ^{13}C NMR spectra were recorded by using a Bruker Avance 300 spectrometer (Bruker, Karlsruhe, Germany) operating at 300 MHz for ^{1}H and 75 MHz for ^{13}C, or using a Bruker Avance 400 spectrometer operating at 400 MHz for ^{1}H and 100 MHz for ^{13}C. IR spectra were measured using a Bruker Alpha-T FTIR spectrometer (Bruker, Ettlingen, Germany). Mass spectra were obtained by using a Thermo Finnigan LCQ Advantage mass spectrometer. Samples for the mass spectrometry were prepared by dissolving the product (2 mg) in methanol (1 mL), then adding this solution (200 μL) to a water/methanol mixture (50:50, 800 μL). The resulting solution was injected at a flow rate of 5 μL min^{-1}. Total X-ray reflection fluorescence (TXRF) measurements were using an S2 Picofox (Bruker, Berlin, Germany) with a molybdenum source. Samples for TXRF were prepared by dissolving the complex (1 mg) in milli-Q H_2O (1 mL). This solution was diluted 10 times, and then this stock solution (500 μL) was mixed with a calculated volume of gallium(III) standard (1000 ppm) so that the lanthanide(III) concentration was similar to the gallium(III) one. Finally, this mixture (10 μL) was placed on a Bruker AXS quartz glass sample plate for measurement. Absorption spectra were measured using a Varian Cary 5000 spectrophotometer on freshly prepared aqua solutions in quartz Suprasil cells (115F-QS) with an optical path length of 0.2 cm. Photophysical data (excitation, emission spectra and lifetimes) were recorded using an Edinburgh Instruments FS920 steady state spectrofluorimeter. This instrument was equipped with a 450 W xenon arc lamp, a high-energy microsecond flashlamp μF900H, and an extended red-sensitive photomultiplier (185–1010 nm, Hamamatsu R 2658P). All spectra are corrected for the instrumental functions. Luminescence lifetimes under ligand excitation for Eu^{III} complexes were measured by monitoring either $^5D_0$→$^7F_2$ (614 nm) or $^5D_0$→$^7F_4$ (695 nm) transitions. They are the

average of at least three independent measurements. Quantum yields were determined by comparative method using a solution of quinine sulfate (Fluka) in 1N H_2SO_4 ($Q = 54.6\%$) as standard; estimated error $\pm 20\%$.[70]

Model: The model was built using Avogadro.[71] The central part that contained Ti^{IV} and three 1,2-dihydroxybenzene molecules and the arms including Gd^{III} were first optimized separately with the universal force field (UFF).[72] The 1,2-dihydroxybenzene parts of the central part and the arms were overlaid and the entire complex was reoptimized with UFF using Open Babel.

^{17}O NMR spectroscopy: ^{17}O NMR spectroscopic measurements of solutions were performed on samples (350 µL) placed in 5 mm external diameter tubes using a Bruker AVANCE-500 spectrometer (Bruker, Karlsruhe, Germany). Temperature was regulated by air or nitrogen flow controlled using a Bruker BVT 3200 unit. ^{17}O transverse relaxation times of distilled water (pH 6.5–7) were measured using a Carr–Purcell–Meiboom–Gill (CPMG) sequence and a subsequent two parameters fit of the data points. The 90 and 180° pulse lengths were 27.5 and 55 µs, respectively. ^{17}O T_2 of water in complex solution was obtained from line-width measurements. All spectra were proton decoupled. The concentration of $[(Gd4)_3Ti(H_2O)_3]^{5-}$ was equal to 3.12 mM (9.37 mM for Gd^{III}). The data are presented as the reduced transverse relaxation rate ($1/T_2^R = 55.55/(T_2^{para} \times q \times [Gd])$), in which [Gd] is the molar concentration of the complexed Gd^{III}, q is the number of coordinated water molecules, and T_2^{para} is the paramagnetic transverse relaxation rate). The treatment of the experimental data was performed as described previously.[60,61]

Proton NMRD: Proton nuclear magnetic relaxation dispersion (NMRD) profiles were measured using a Stelar Spinmaster FFC (fast field cycling) NMR relaxometer (Stelar, Mede (PV), Italy) over a magnetic field strength range that extended from 0.24 mT to 0.7 T. Measurements were performed on 0.6 mL samples contained in 10 mm (outside diameter) pyrex tubes. Additional relaxation rates at 20, 60, and 300 MHz were respectively obtained using a Minispec mq20, a Minispec mq60, and a Bruker AVANCE-300 spectrometer (Bruker, Karlsruhe, Germany). The proton NMRD curves were fitted using data-processing software,[73,74] including different theoretical models that describe the nuclear relaxation phenomena (Minuit, CERN Library).[57–59]

Acknowledgements

This work was financially supported by the ARC (research contract AUWB-2010-10/15 UMONS-5), FNRS and ENCITE. Programs for Research of the French Community of Belgium, and it was performed in the framework of COST D38 (Metal-Based Systems for Molecular Imaging Applications) and the European Network of Excellence EMIL (European Molecular Imaging Laboratories) program LSCH-2004-503569. The authors thank the Center for Microscopy and Molecular Imaging (CMMI, supported by the European Regional Development Fund and the Walloon Region). G.D., T.N.P.V., and K.B. acknowledge the I.W.T. Flanders (Belgium) and the FWO-Flanders (project G.0412.09) for financial support. S.V.E. is a visiting postdoctoral fellow of the FWO-Flanders (project G.0412.09). CHN microanalysis was performed by Mr. Dirk Henot. ESI-MS measurements were made by Mr. Dirk Henot and Mr. Bert Demarsin, and ICP-MS measurements were performed by Ms. Solvita Ore (Department of Chemical Engineering). Mr. Karel Duerinckx is acknowledged for his help in the NMR spectroscopic measurements. We also thank Mr. Servaas Michielssens for his development of the framework molecular model.

[1] P. Caravan, J. J. Ellison, T. J. McMurry, R. B. Lauffer, *Chem. Rev.* **1999**, *99*, 2293–2352.
[2] *The Chemistry of Contrast Agents in Medical Magnetic Resonance Imaging*, (Eds.: A. E.Merbach, E.Tóth), Wiley, London, **2001**.
[3] L. Moriggi, A. Aebischer, C. Cannizzo, A. Sour, A. Borel, J.-C. G. Bünzli, L. Helm, *Dalton Trans.* **2009**, 2088–2095.
[4] S. Aime, M. Botta, M. Fasano, E. Terreno, *Chem. Soc. Rev.* **1998**, *27*, 19–29.
[5] J. Kowalewski, L. Nordenskiöld, N. Benetis, P. O. Westlund, *Prog. Nucl. Magn. Reson. Spectrosc.* **1985**, *17*, 141–185.
[6] P. Caravan, *Chem. Soc. Rev.* **2006**, *35*, 512–523.
[7] T. M. Grist, F. R. Korosec, D. C. Peters, S. Witte, R. C. Walovitch, R. P. Dolan, W. E. Bridson, E. K. Yucel, C. A. Mistretta, *Radiology* **1998**, *207*, 539–544.
[8] R. B. Lauffer, D. J. Parmelee, H. S. Ouellet, R. P. Dolan, H. Sajiki, D. M. Scott, P. J. Bernard, E. M. Buchanan, K. Y. Ong, Z. Tycklar, K. S. Midelfort, T. J. McMurry, *Acad. Radiol.* **1996**, *3*, S356-S358.
[9] P. Caravan, N. J. Cloutier, M. T. Greenfield, S. A. McDermid, S. U. Dunham, J. W. M. Bulte, J. C. Amedio, R. J. Looby, R. M. Supkowski, W. D. Horrocks Jr., T. J. McMurry, R. B. Lauffer, *J. Am. Chem. Soc.* **2002**, *124*, 3152–3162.
[10] T. Parac-Vogt, K. Kimpe, S. Laurent, C. Pierart, L. Vander Elst, R. N. Muller, K. Binnemans, *Eur. Biophys. J.* **2006**, *35*, 136–144.
[11] P. L. Anelli, L. Lattuada, V. Lorusso, M. Schneider, H. Tournier, F. Uggeri, *Magn. Reson. Mater. Phys. Biol. Med.* **2001**, *12*, 114–120.
[12] T. N. Parac-Vogt, K. Kimpe, S. Laurent, C. Pierart, L. Vander Elst, R. N. Muller, K. Binnemans, *Eur. J. Inorg. Chem.* **2004**, 3538–3543.
[13] J. B. Livramento, E. Toth, A. Sour, A. Borel, A. E. Merbach, R. Ruloff, *Angew. Chem.* **2005**, *117*, 1504–1508; *Angew. Chem. Int. Ed.* **2005**, *44*, 1480–1484.
[14] J. B. Livramento, C. Weidensteiner, M. I. M. Prata, P. R. Allegrini, C. F. G. C. Geraldes, L. Helm, R. Kneuer, A. E. Merbach, A. C. Santos, P. Schmidt, E. Toth, *Contrast Media Mol. Imaging* **2006**, *1*, 30–39.
[15] J. B. Livramento, A. Sour, A. Borel, A. E. Merbach, E. Toth, *Chem. Eur. J.* **2006**, *12*, 989–1003.
[16] V. Jacques, J. F. Desreux, *Top. Curr. Chem.* **2002**, *221*, 123–164.
[17] V. Comblin, D. Gilsoul, M. Hermann, V. Humblet, V. Jacques, M. Mesbahi, C. Sauvage, J. F. Desreux, *Coord. Chem. Rev.* **1999**, *185–186*, 451–470.
[18] M. J. Kappel, K. N. Raymond, *Inorg. Chem.* **1982**, *21*, 3437–3442.
[19] B. A. Borgias, S. R. Cooper, Y. B. Koh, K. N. Raymond, *Inorg. Chem.* **1984**, *23*, 1009–1016.
[20] L. Sommer, *Collect. Czech. Chem. Commun.* **1963**, *28*, 2102–2130.
[21] C. Creutz, M. H. Chou, *Inorg. Chem.* **2008**, *47*, 3509–3514.
[22] W. Macyk, K. Szacilowski, G. Stochel, M. Buchalska, J. Kuncewicz, P. Labuz, *Coord. Chem. Rev.* **2010**, *254*, 2687–2701.
[23] M. J. Sever, J. J. Wilker, *Dalton Trans.* **2004**, 1061–1072.
[24] M. J. Sever, J. J. Wilker, *Dalton Trans.* **2006**, 813–822.
[25] C. S. Bonnet, E. Toth, *Comptes Rendus Chim.* **2010**, *13*, 700–714.
[26] L. Frullano, T. J. Meade, *J. Biol. Inorg. Chem.* **2007**, *12*, 939–949.
[27] S. Laurent, L. Vander Elst, R. N. Muller, *Quart. J. Nucl. Med. Mol. Imaging* **2009**, *53*, 586–603.
[28] A. Louie, *Chem. Rev.* **2010**, *110*, 3146–3195.
[29] M. Modo, D. Cash, K. Mellodew, S. C. R. Williams, S. E. Fraser, T. J. Meade, J. Price, H. Hodges, *NeuroImage* **2002**, *17*, 803–811.
[30] Y. Song, H. Zong, E. R. Trivedi, B. J. Vesper, E. A. Waters, A. G. M. Barrett, J. A. Radosevich, B. M. Hoffman, T. J. Meade, *Bioconjugate Chem.* **2010**, *21*, 2267–2275.
[31] M. M. Hüber, A. B. Staubli, K. Kustedjo, M. H. B. Gray, J. Shih, S. E. Fraser, R. E. Jacobs, T. J. Meade, *Bioconjugate Chem.* **1998**, *9*, 242–249.
[32] T. Koullourou, L. S. Natrajan, H. Bhavsar, S. J. A. Pope, J. H. Feng, J. Narvainen, R. Shaw, E. Scales, R. Kauppinen, A. M. Kenwright, S. Faulkner, *J. Am. Chem. Soc.* **2008**, *130*, 2178–2179.
[33] J. Shen, L. D. Sun, Y. W. Zhang, C. H. Yan, *Chem. Commun.* **2010**, *46*, 5731–5733.
[34] P. Howes, M. Green, A. Bowers, D. Parker, G. Varma, M. Kallumadil, M. Hughes, A. Warley, A. Brain, R. Botnar, *J. Am. Chem. Soc.* **2010**, *132*, 9833–9842.
[35] W. J. Rieter, J. S. Kim, K. M. L. Taylor, H. Y. An, W. Lin, T. Tarrant, W. Lin, *Angew. Chem.* **2007**, *119*, 3754–3756; *Angew. Chem. Int. Ed.* **2007**, *46*, 3680–3682.
[36] P. L. Anelli, F. Fedeli, O. Gazzotti, L. Lattuada, G. Lux, F. Rebasti, *Bioconjugate Chem.* **1998**, *9*, 137–140.

[37] C. F. G. C. Geraldes, A. M. Urbano, M. A. Hoefnagel, J. A. Peters, *Inorg. Chem.* **1993**, *32*, 2426–2432.
[38] M. Albrecht, S. Mirtschin, M. de Groot, I. Janser, J. Runsink, G. Raabe, M. Kogej, C. A. Schalley, R. Fröhlich, *J. Am. Chem. Soc.* **2005**, *127*, 10371–10387.
[39] J. L. Martin, J. Takats, *Can. J. Chem.* **1975**, *53*, 572–577.
[40] R. Uppal, H.P Israel, C. C. Incarvito, A. M. Valentine, *Inorg. Chem.* **2009**, *48*, 10769–10779.
[41] J.-C. G. Bünzli, S. V. Eliseeva, in *Lanthanide Luminescence: Photophysical, Analytical and Biological Aspects (Springer Series on Fluorescence)*, *Vol 7*, (Eds.: P. Hänninen, H. Härmä), Springer Verlag, Berlin, **2011**, pp. 1–45.
[42] A. D'Aléo, M. Allali, A. Picot, P. L. Baldeck, L. Toupet, C. Andraud, O. Maury, *Comptes Rendus Chim.* **2010**, *13*, 681–690.
[43] L. L. Pesterfield, N. A. Stump, *Spectrosc. Lett.* **1997**, *30*, 47–59.
[44] G. Vereb, E. Jares-Erijman, P. R. Selvin, T. M. Jovin, *Biophys. J.* **1998**, *74*, 2210–2222.
[45] R. M. Supkowski, W. D. Horrocks Jr., *Inorg. Chim. Acta* **2002**, *340*, 44–48.
[46] M. Vázquez López, S. V. Eliseeva, J. M. Blanco, G. Rama, M. R. Bermejo, M. E. Vazquez, J.-C. G. Bünzli, *Eur. J. Inorg. Chem.* **2010**, 4532–4545.
[47] S. Petoud, J.-C. G. Bünzli, T. Glanzman, C. Piguet, Q. Xiang, R. P. Thummel, *J. Lumin.* **1999**, *82*, 69–79.
[48] L. N. Puntus, K. A. Lyssenko, I. Pekareva, J.-C. G. Bünzli, *J. Phys. Chem. B* **2009**, *113*, 9265–9277.
[49] G. Murali Krishna, Y. Gandhi, N. Veeraiah, *J. Lumin.* **2008**, *128*, 631–634.
[50] Y. Hizhnyi, A. Oliynyk, O. Gomenyuk, S. Nedilko, P. Nagornyi, R. Boiko, V. Boyko, *Mater. Sci. Eng. B* **2007**, *144*, 7–10.
[51] S. Nedilko, Y. Hizhnyi, O. Chukova, P. Nagornyi, R. Bojko, V. Boyko, *J. Nucl. Mater.* **2009**, *385*, 479–484.
[52] T. Yamashita, K. Ueda, *J. Solid State Chem.* **2007**, *180*, 1410–1413.
[53] M. C. Carotta, S. Gherardi, V. Guidi, C. Malagu, G. Martinelli, B. Vendemiati, M. Sacerdoti, G. Ghiotti, S. Morandi, A. Bismuto, P. Maddalena, A. Setaro, *Sens. Actuators B* **2008**, *130*, 38–45.
[54] A. T. Tashkhodzhaev, L. E. Zel'tser, T. Sabirova, L. A. Morozova, *Dokl. Akad. Nauk UzSSR* **1976**, 32–33.
[55] A. Strasser, A. Vogler, *Inorg. Chim. Acta* **2004**, *357*, 2345–2348.
[56] J.-P. Cornard, C. Lapouge, C. Allet-Bodelot, *Chem. Phys. Lett.* **2010**, *489*, 164–168.
[57] I. Solomon, *Phys. Rev.* **1955**, *99*, 559–565.
[58] N. Bloembergen, *J. Chem. Phys.* **1957**, *27*, 572–573.
[59] J. H. Freed, *J. Chem. Phys.* **1978**, *68*, 4034–4037.
[60] R. N. Muller, B. Raduchel, S. Laurent, J. Platzek, C. Pierart, P. Mareski, L. Vander Elst, *Eur. J. Inorg. Chem.* **1999**, 1949–1955.
[61] S. Laurent, L. V. Houze, N. Guerit, R. N. Muller, *Helv. Chim. Acta* **2000**, *83*, 394–406.
[62] F. Botteman, G. M. Nicolle, L. Vander Elst, S. Laurent, A. E. Merbach, R. N. Muller, *Eur. J. Inorg. Chem.* **2002**, 2686–2693.
[63] K. Micskei, L. Helm, E. Brucher, A. E. Merbach, *Inorg. Chem.* **1993**, *32*, 3844–3850.
[64] G. Gonzalez, D. H. Powell, V. Tissieres, A. E. Merbach, *J. Phys. Chem.* **1994**, *98*, 53–59.
[65] L. Vander Elst, F. Maton, S. Laurent, F. Seghi, F. Chapelle, R. N. Muller, *Magn. Reson. Med.* **1997**, *38*, 604–614.
[66] L. Vander Elst, A. Sessoye, S. Laurent, R. N. Muller, *Helv. Chim. Acta* **2005**, *88*, 574–587.
[67] S. Laurent, L. Vander Elst, F. Botteman, R. N. Muller, *Eur. J. Inorg. Chem.* **2008**, 4369–4379.
[68] C. M. Micklitsch, Q. Yu, J. P. Schneider, *Tetrahedron Lett.* **2006**, *47*, 6277–6280.
[69] P. L. Anelli, F. Fedeli, O. Gazzotti, L. Lattuada, G. Lux, F. Rebasti, *Bioconjugate Chem.* **1999**, *10*, 137–140.
[70] D. F. Eaton, *Pure Appl. Chem.* **1988**, *60*, 1107–1114.
[71] Avogadro: an open-source molecular builder and visualization tool. Version 1.0.0. http://avogadro.openmolecules.net/. 2011.
[72] A. K. Rappe, C. J. Casewit, K. S. Colwell, W. A. Goddard, W. M. Skiff, *J. Am. Chem. Soc.* **1992**, *114*, 10024–10035.
[73] R. N. Muller, D. Declercq, P. Vallet, F. Giberto, B. Daminet, H. W. Fischer, F. Maton and Y. Van Haverbeke, *Proceedings of ESMRMB, 7th Annual Congress*, Strasbourg, **1990**, 394.
[74] P. Vallet, Relaxivity of Nitroxide Stable Free Radicals. Evaluations by Field Cycling Method and Optimisation, PhD dissertation, University of Mons-Hainaut, Belgium, **1992**.

Received: May 9, 2011
Revised: August 23, 2011
Published online: ■■ ■■, 0000

Let's get photophysical: This work deals with the design and investigation of relaxometric and photophysical properties of a self-assembled supramolecular complex that contains three Ln-DTPA-catechol (DTPA = diethylenetriamine-*N*,*N*,*N*′,*N*″,*N*″-pentaacetate) moieties around a central Ti^{IV} core (see figure).

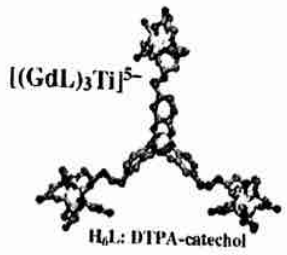

Supramolecular Complexes

*G. Dehaen, S. V. Eliseeva, K. Kimpe, S. Laurent, L. Vander Elst, R. N. Muller, W. Dehaen, K. Binnemans, T. N. Parac-Vogt** ..... ▮▮▮▮–▮▮▮▮

A Self-Assembled Complex with a Titanium(IV) Catecholate Core as a Potential Bimodal Contrast Agent

